Giant magnetoresistance in bulk mechanically alloyed Co-Ag

1995 J. Phys.: Condens. Matter 7 8953

(http://iopscience.iop.org/0953-8984/7/47/015)

J. Phys.: Condens. Matter 7 (1995) 8953–8966. Printed in the UK

Giant magnetoresistance in bulk mechanically alloyed Co–Ag

A J Fagan, M Viret and J M D Coey
Department of Physics, Trinity College, Dublin 2, Ireland

Received 23 March 1995, in final form 24 July 1995

Abstract. Bulk granular magnetic solids have been prepared by the high-energy mechanical alloying of fine cobalt and silver powders, with cobalt concentrations of 5, 15 and 30 at.%. The threshold for giant magnetoresistance in the parent samples was found to lie between 5 and 15 at.% Co, with a maximum effect of 12% at 4 K in the 30 at.% Co sample. The effect of the mechanical alloying process parameters, such as the milling energy, milling time and annealing, on the magnitude of the GMR in this system was also investigated. The sub-micron scale homogeneity of the samples was found to vary with the milling energy, with completely homogeneous samples produced after milling at high energy, and only 60% homogeneity levels achieved in the sample milled at a lower energy. The isotropic and anisotropic contributions to the total magnetoresistance were separated experimentally, and the linear relationship between the two (derived for an ideal superparamagnetic system) was observed experimentally.

1. Introduction

The observation of giant negative magnetoresistance (GMR) in nanostructured granular magnetic systems, consisting of nanometer-sized granules of a 3d ferromagnetic element dispersed in a non-magnetic, metallic matrix, is a recent result [1]. Intense experimental and theoretical work on GMR carried out over the past decade has been motivated partly by the potential of these materials for applications in the information storage industry, but also by a desire to understand the underlying mechanisms responsible for the anomalous magnetotransport [2]. The giant magnetoresistance in granular systems is an isotropic effect, which is typically an order of magnitude or more greater than the anisotropic magnetoresistance (AMR) due to spin–orbit coupling.

The recent interest in negative magnetoresistance effects stems from observations in multilayers systems, such as Fe–Cr, where the different scattering probabilities of spin-up and spin-down electrons lead to the GMR, attributed to the reorientation of monodomain magnetic layers [3]. The associated of GMR with the ability to change the relative orientation of magnetic domains led to the investigation of GMR in granular magnetic systems. Here, the spin-dependent scattering responsible for the GMR originates from the alignment of single-domain grains, with the maximum scattering (and hence resistivity) occurring when there is the greatest degree of magnetic misalignment. A much earlier observation of GMR was reported in the vicinity of the Curie temperature of manganate perovskites with the general formula $(La_{1-x}A_x)$ Mn O_3 with A = Ca, Ba, Sr, Pb [4]. There, it results from the effect of a magnetic field on the spin-dependent scattering of the conduction electrons from fluctuating regions of correlated magnetization [5].

Granular magnetic systems exhibiting GMR have been produced in thin film form by the sputtering and subsequent annealing of immiscible elements such as Fe–Cu, Co–Cu and Co–Ag [6, 7], and also in annealed melt-spun Co–Cu ribbons [8]. More recently, we extended the observation of GMR in granular systems to bulk material, finding values in

0953-8984/95/478953+14$19.50

excess of 10% at 4.2 K in mechanically-alloyed Co–Ag [9]. The Co–Ag system is ideal for studying the GMR effect, because the elements are immiscible in all proportions, forming no intermetallic compounds and having no significant range of solid solution. Furthermore, cobalt is a strong ferromagnet, with a fully spin polarized 3d band which enhances the effects of spin-dependent scattering.

The focus of this paper is an investigation of the effect of the mechanical alloying process parameters, such as the milling energy, the milling time and subsequent heat treatments, on the magnitude of the GMR in this system. The distribution of cobalt particle size is modelled. The anisotropic AMR and isotropic GMR terms are separated experimentally and the relationship between them is discussed.

2. Experimental methods

Ten-grain mixtures of pure fine powders (Ag—99.9%, 2–3 μm; Co—99.8%, < 2 μm) were prepared with varying Co concentrations of 10, 15 and 30 at.% in a glovebox with an argon atmosphere with < 1 ppm H_2O and O_2. They were subsequently mechanically alloyed with 170 g of 10 mm stainless steel ball bearings in a Fritsch PM5 Planetary ball mill for 42 h at the maximum energy (corresponding to 300 revolutions per minute (rpm) about the central axis and 540 rpm about each individual pot axis). The 30 at.% Co composition was also milled at half of the maximum energy for 42, 65, 86 and 130 h. Approximately 7–8 g of free, coarse powder with a particle size ranging from ~ 50 μm to 1 mm was recovered from each milling experiment. Heat treatments were carried out on the 30 at.% Co sample milled at high energy. In each case, the sample was heated to 150, 250, 350 and 500 °C for one hour in a vacuum of 10^{-2} mbar.

Microstructural investigation of the samples was carried out in a scanning electron microscopy (SEM), with a chemical analysis by energy dispersive x-ray scattering providing information on the composition of the milled materials. Structural analysis by x-ray diffraction was carried out using a Siemens Diffrac 500 diffractometer with Cu Kα radiation. The 30 at.% samples milled at high and low energy were also studied using a high-resolution Philips diffractometer with Fe Kα radiation.

Magnetization measurements were carried out on samples of ~ 10 mg using a compact permanent-magnet vibrating-sample magnetometer (VSM) at room temperature [10] and a conventional superconducting electromagnet VSM at 4.2 K. Electrical measurements were conducted on foils between 3 and 10 mm^2 by $\sim 100$$\mu$m thick, obtained by squashing a large single grain under an applied pressure of 800 MPa. Four contacts were made with high conductivity silver paint and 50 μm silver wire in the Van der Pauw geometry [11]. A linear research LR400 ac resistance bridge set-up was used to measure the magnetoresistance, with measurements being made up to 1.4 T at room temperature in all three orientations of the current with respect to the applied field.

3. Results

No inhomogeneity was detected in the SEM for the samples milled at high energy. However, in the low-energy milled samples both homogeneous and inhomogeneous regions were seen to co-exist on a micron scale, the latter consisting of micron-sized Co-rich areas dispersed in a Ag-rich matrix. Furthermore, the amount of sample in the homogeneous regions increased from $\sim 40\%$ to $\sim 60\%$ for milling times of 42 and 130 h respectively. In the SEM micrograph of figure 1(b), a boundary between two such regions is shown, together with one of the same composition milled at higher energy in figure 1(a). No change in

the microstructure of the high-energy milled samples was observed after annealing. In all samples, the amount of iron impurity due to contamination by the steel milling pots and balls was found to be less than 1%, while the starting Co:Ag ratio was maintained for all but the 10 at.% Co sample milled at high energy, for which the final Co concentration in the milled powder was found to fall to 5 at.%.

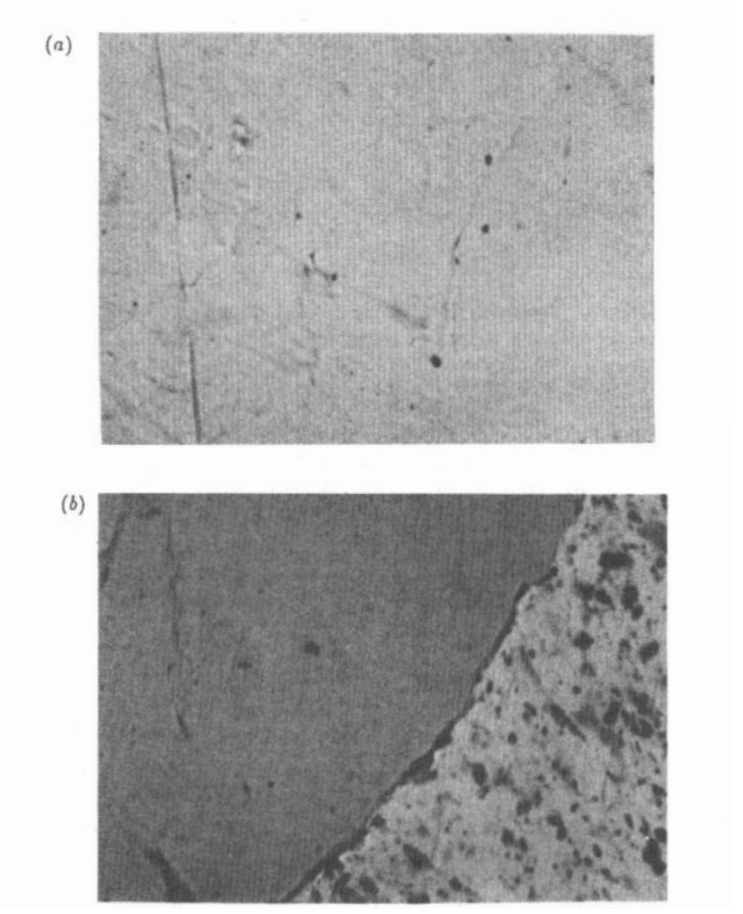

Figure 1. SEM micrographs taken at a magnification of 2 K (20 μm × 30 μm) for the $Co_{30}Ag_{70}$ samples milled at (a) high energy and (b) low energy for 130 h. A boundary between a homogeneous and in inhomogeneous region is shown for the low-energy sample in (b). The black areas are Co rich.

The 30 at.% sample milled at high energy exhibited broad phase-separated x-ray diffraction peaks corresponding to small fcc Co grains embedded in a fcc Ag matrix. No Co peaks could be observed in the diffraction patterns of the 15 and 5 at.% samples. A similar phase separation was evident in the low-energy milled samples, although there the hcp Co structure was found to exist, with only a very weak (200) reflection of the fcc phase after milling for 130 h. The broad diffraction peaks for each element are indicative of both crystalline size and strain broadening effects with the Ag lattice parameter shifted toward that of Co, and vice-versa. These effects all decreased with increasing annealing temperature. Figure 2 shows the diffraction patterns of the 30 at.% Co samples milled at low energy for 130 h, and at high energy for 42 h before and after annealing at 500 °C.

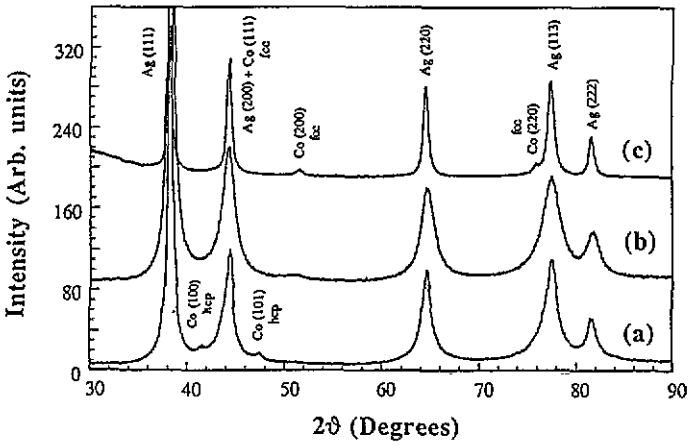

Figure 2. The x-ray diffraction pattern using Cu Kα radiation for the $Co_{30}Ag_{70}$ samples milled at (a) low energy for 130 h, and at high energy for (b) the parent material and (c) after annealing at 500 °C. Both (b) and (c) were shifted vertically for clarity.

The higher resolution of the Philips diffractometer succeeded in resolving two components in each of the Ag diffraction peaks, except the (111) peak, for the 30 at.% sample milled at high energy (figure 3). The sharper, higher-angle component with $a_0 = 0.4068$ nm may correspond to a metastable solid solution of Co in Ag, possibly located in a halo around the Co grains. An application of Vegard's law to the decrease in lattice parameter suggests that the cobalt content there is $\sim 3\%$.

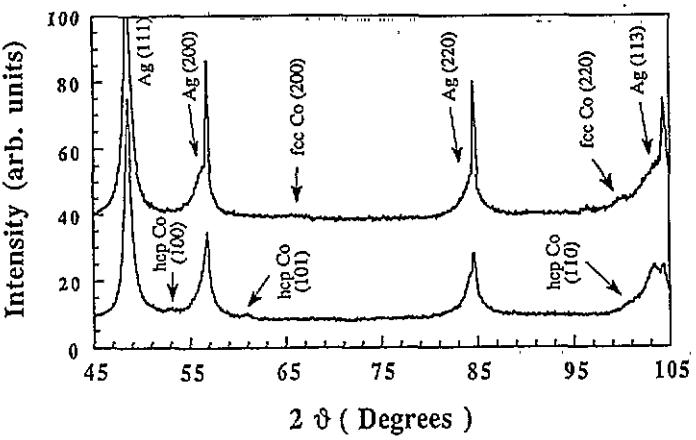

Figure 3. The x-ray diffraction pattern using Fe Kα radiation for the $Co_{30}Ag_{70}$ sample milled at (a) high energy and (b) low energy for 130 h (shifted vertically for clarity). Both spectra show evidence for a metastable solid solution of Co in Ag, probably located in a halo around the Co crystallites.

Room temperature magnetoresistance curves for the high-energy milled $Co_{30}Ag_{70}$ sample are shown in figure 4 for the perpendicular, longitudinal and transverse geometries. In granular systems, the giant magnetoresistance is expected to be isotropic [6]. The broader hysteresis in the perpendicular geometry can be ascribed to the demagnetizing effect, while

the smaller change in resistivity for the longitudinal geometry is a direct consequence of the anisotropic magnetoresistance effect (AMR), which becomes more evident when the GMR is small. The resistivity was measured to be 14.1×10^{-8} Ωm (typical values were between 10–25 $\times 10^{-8}$ Ωm) and decreased by 3.2–4.2% in 1.4 T, depending on the direction of the current with respect to the field. As shown in table 1, the GMR decreased with decreasing Co concentration, with the threshold composition lying between 5 and 15 at.% Co.

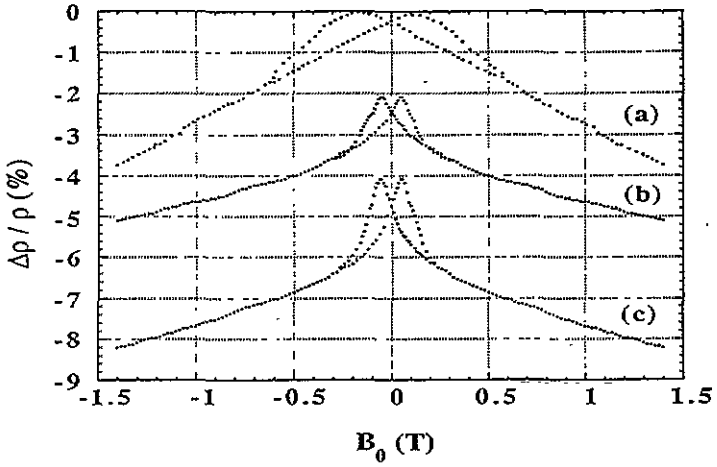

Figure 4. The room temperature magnetoresistance of the high-energy milled $Co_{30}Ag_{70}$ sample in the (a) perpendicular, (b) longitudinal and (c) transverse geometries.

Table 1. The room temperature data for the 5, 15 and 30 at.% Co samples milled at high energy. The remanent magnetization, σ_r, is given as a fraction of σ(1.4 T). B_c is the coercivity d_{111} is the effective crystallite size, determined from the Ag(111) peak (a_0/pure Ag = 0.4086 nm; a_0/pure fcc Co = 0.3544 nm).

at/% Co	a_0 Ag (nm)	d_{111} Ag (nm)	GMR (%)	σ(1.4 T)	σ_r/σ	B_c (mT)
5	0.4079	16.3	< 0.1	7.7	0.12	31
15	0.4082	11.4	3.1	15.0	0.09	52
30	0.4082	7.8	4.2	29.4	0.30	55

The average size (d_{111}) of the Ag crystallites was determined in each case from an application of the Scherrer formula to the width of the Ag(111) Cu Kα x-ray diffraction peaks. Similarly, from the width of the fcc Co (200) peak, the Co crystallite size for the $Co_{30}Ag_{70}$ sample was estimated to be of the order of 5 nm.

The room temperature magnetization of each sample in 1.4 T is between 10 and 20% less than the saturation magnetization expected from the Co content, due to the presence of superparamagnetic grains which are not saturated in this field. Furthermore, any cobalt entering a metastable solid solution in Ag will not contribute to the magnetization. Nevertheless, the relatively large coercive fields imply that a significant fraction of grains are blocked at room temperature, which indicates that the grain size distribution in these materials covers the critical size for blocking, which may be ~ 5 nm for fcc cobalt [12].

In order to estimate the size spread of the Co grains, the magnetization curve for the homogeneous $Co_{30}Ag_{70}$ sample milled at high energy was fitted to a function comprising

of both a superparamagnetic (SP) and a ferromagnetic (FM) component for several particle volume distributions. The experimental curves can be fitted well with several distribution shapes. Because of the lack of an idea to justify any particular distribution of Co grains in these materials, we chose the very simple distribution function consisting of a constant particle volume density between two limits: v_m and v_M (figure 5). The expression of the superparamagnetic part of the magnetization is:

$$M_{sp}(B_0) = \frac{M_s}{(v_b - v_m)\alpha'} \cdot \ln\left[\frac{v_m \sinh(\alpha' v_b)}{v_b \sinh(\alpha' v_m)}\right]$$

where M_s is the saturation magnetization for the superparamagnetic part, v_m is the minimum volume of the distribution and v_b is the blocking volume, beyond which the particle behaves like a normal ferromagnet (not in the superparamagnetic regime), and α' is the magnetothermal ratio

$$\alpha' = \frac{\mu'}{kT} B_0$$

where μ' is the average moment per Co atom of the grains in the superparamagnetic regime. In order to determine the other parameter of the distribution, v_M, we can express the ratio of the saturation magnetizations of the ferromagnetic and the superparamagnetic parts as follows:

$$\frac{M_F}{M_s} = \frac{vM^2 - vb^2}{vb^2 - vm^2}.$$

Thus, all the parameters of interest for the grain size distribution can be obtained without having to fit the shape of the ferromagnetic magnetization. However, in order to compare the final theoretical magnetization curves to the corresponding data, we choose to use the loop function from [13] for the ferromagnetic part. The fit shown in figure 5, yields a superparamagnetic fraction of 68% with $M_s = 20.9$ J(T kg)$^{-1}$, $v_m = 4.65$ nm^3, $v_b = 80.3$ nm^3, $v_M = 114$ nm^3.

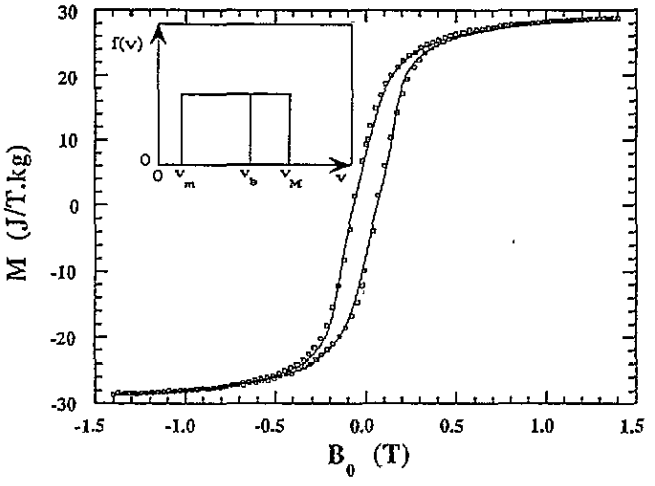

Figure 5. A fit of the room temperature magnetization curve of the $Co_{30}Ag_{70}$ sample milled at high energy. The inset shows the particle size distribution used for the fit.

As expected, the spread of Co particle size is rather large in the parent compound and the minimum volume obtained for the distribution corresponds to an aggregate of only about 200 atoms. It is interesting to check how the size distribution changes after annealing. The same analysis when then carried out on the sample annealed at 500 °C. The superparamagnetic fraction was found to be 90% with $M_s = 29$ J(T kg)$^{-1}$, $v_m = 26.9$ nm^3, $v_b = 81.7$ nm^3 and $v_M = 85.7$ nm^3. The distribution is much narrower than in the parent alloy, and only a small number of Co grains are above the blocking volume. Also, the fact that the value of v_b given by the fit is very close to that obtained for the previous curve gives us confidence that this distribution function, although simple, it adequate to describe our granular system. The analysis also leads to the determination of the blocking volume for Co grains as 80 nm^3, which by considering the grains to be spherical leads to a blocking diameter of 5.4 nm. It is interesting that the maximum volume obtained with the square distribution decreases after the first anneal. This result might be explained in terms of the large density of defects induced by the ball-milling process in the parent compound. Upon annealing, silver may penetrate the grain boundaries and separate the Co grains into smaller and more spherical particles. A similar effect has been observed in discontinuous multilayers in which post-annealing treatments create pancake-like Co particles [14] which behave in a superparamagnetic manner. Also, spherical particles will behave in a more superparamagnetic way than those which show some degree of shape anisotropy. Upon further annealing, the maximum volume for Co grains was observed to increase, as expected for the Co/Ag system.

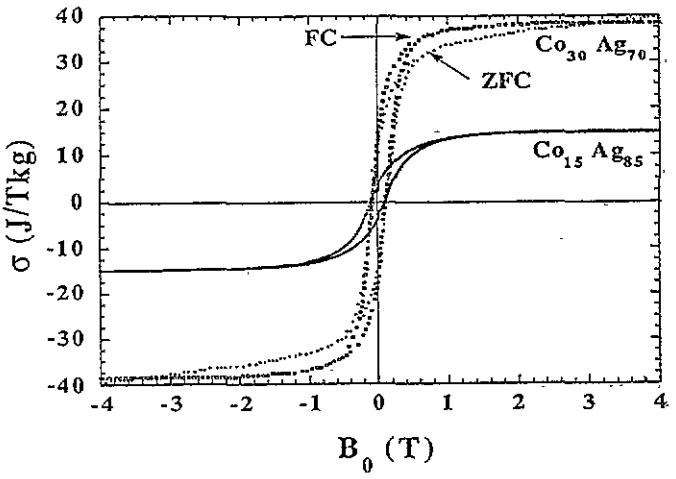

Figure 6. Hysteresis loops of the high-energy milled $Co_{30}Ag_{70}$ and $Co_{15}Ag_{85}$ samples measured at 4.2 K, showing the field-cooled (FC) and zero-field-cooled (ZFC) behaviour of the $Co_{30}Ag_{70}$ sample.

The 4.2 K magnetization curves for the 15 and 30 at.% samples are shown in figure 6. The magnetization of the 30 at.% sample showed considerable sensitivity to its thermal history, saturating more easily after field cooling to 4.2 K in 5 T. Furthermore, the saturation magnetization increases significantly compared to its room temperature value. No such effects were found in the 15 at.% sample, for which the field-cooled and zero-field-cooled magnetizations saturated in the same field.

Table 2 summarizes the effects of annealing on the properties of the $Co_{30}Ag_{70}$ sample milled at high energy. As expected, a large increase in both the Ag and Co crystallite

Table 2. The effects of annealing on the properties of the $Co_{30}Ag_{70}$ sample milled at high energy. T_A is the annealing temperature.

					295 K				4 K			
T_A (°C)	a_0–Ag (nm)	d_{111}–Ag (nm)	a_0–Co (nm)	d_{200}–Co (nm)	GMR (%) 1.4 T	σ(1.4 T) (J(T kg)$^{-1}$)	σ_r/σ	B_c (mT)	GMR (%) 4 T	σ(1.4 T) (J(T kg)$^{-1}$)	σ_r/σ	B_c (mT)
150	0.40828	8.8	0.3561	5.0	3.9	29.4	0.28	56				
250	0.40851	9.7	0.3599	5.5	3.4	29.8	0.27	52	13.0	33.5	0.47	128
350	0.40868	11.6	0.3558	6.8	3.2	30.4	0.22	51	12.5			69
500	0.40862	18.0	0.3551	9.0	1.0	30.4	0.16	44				

sizes was found for higher annealing temperatures. Evidence of the exsolution of the cobalt from the metastable Co–Ag solid solution at high annealing temperatures can be seen in the progressive shift of both the Co and the Ag lattice parameters towards the pure metal values, and also in the slight increase in the room temperature magnetization. A concurrent reduction in both remanent magnetization and coercive field were also found, which can be attributed to a reduction of the weak magnetic interactions which were found to exist between the Co grains in the parent material [15].

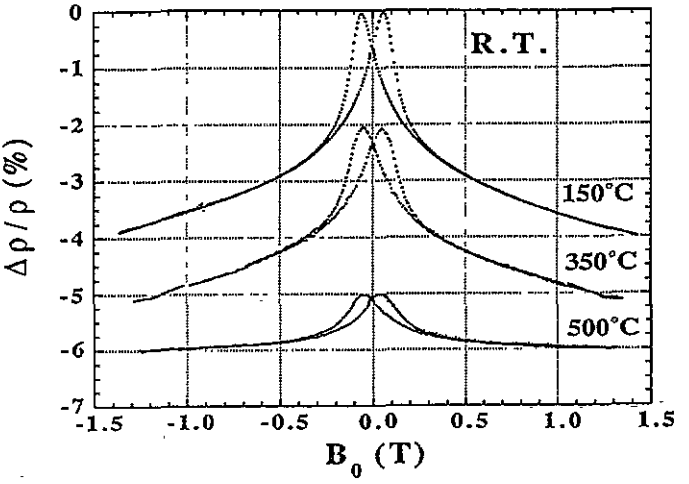

Figure 7. The room temperature transverse magnetoresistance of the high-energy milled $Co_{30}Ag_{70}$ sample annealed at 150 °C, 250 °C and 500 °C. The latter curves have been shifted vertically by 2 and 4% respectively for clarity.

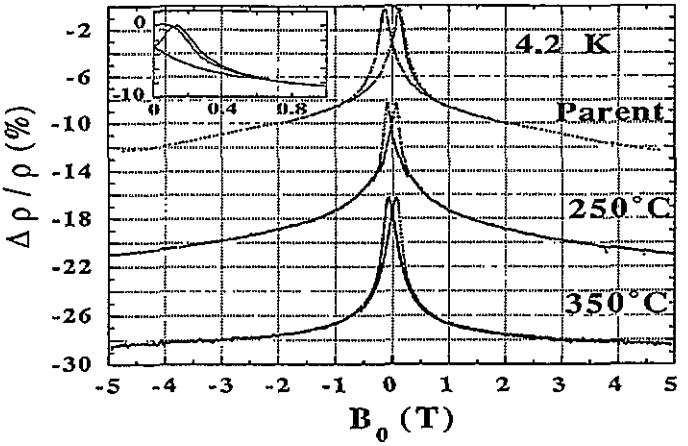

Figure 8. The transverse magnetoresistance at 4.2 K of the high-energy milled $Co_{30}Ag_{70}$ sample before and after annealing at 250 °C and 350 °C. The latter curves have been shifted vertically by 8 and 16% respectively, for clarity. The insert shows the virgin magnetoresistance curve of the parent sample.

The decrease of the GMR with increasing annealing temperature is indicative of the growth, above the optimum size for GMR, of those Co grains which contributed to the GMR in the parent material. The room temperature transverse magnetoresistance curves for the $Co_{30}Ag_{70}$ sample annealed at 150, 350 and 500 °C are shown in figure 7. The progressive reduction in the superparamagnetic fraction in this material is evident both in these curves and in those recorded at 4.2 K, which are shown in figure 8. It is interesting to note that, although the room temperature GMR decreased with increasing annealing temperature, at 4.2 K the GMR peaked after annealing at 250 °C. This may be due to the different temperature dependences of the magnetic and non-magnetic contributions to the scattering.

Table 3. The effects of milling time on the properties of the low-energy milled $Co_{30}Ag_{70}$ sample.

Milling time (h)	a_0–Ag (nm)	d_{111}–Ag (nm)	GMR (295 K) (%)	σ(1.4 T) (J(T kg)$^{-1}$)	σ_r/σ	B_c (mT)
44	0.408 40.	10.6	2.7	29.0	20	38
65	0.408 23	9.6	3.9	29.4	20	37
86	0.408 16	13.9	3.6	28.7	20	38
130	0.408 13	7.2	4.0	29.6	20	39

Table 3 summarizes the data recorded on the low-energy milled sample as a function of milling time. For longer milling times the Ag lattice parameter shifts progressively from the pure Ag value, which suggests the progressive growth of the metastable solid solution with increased milling time. Indeed, even after milling for 130 h, one can see from the x-ray diffraction pattern of figure 3 that the intensity of the diffraction peaks for this phase relative to those of the pure Ag component are significantly lower than those found for the same composition milled at high energy (compare the Ag(113) reflection, for example), suggesting that high-energy milling conditions are favourable for the formation of this metastable solid solution.

4. Discussion

The only evidence for magnetic interactions between neighbouring Co grains was found for the $Co_{30}Ag_{70}$ sample milled at high energy, for which the measured magnetization was found to depend on its thermomagnetic history (figure 6). Another manifestation of these interactions was seen in the magnetoresistance curves, for example in the inset of figure 8. Gregg *et al* [16] have shown that one can determine the net sign of the interactions from the difference between $\Delta\rho/\rho$ for the virgin curve and subsequent field-sweep curves, which in this case is negative, indicating antiferromagnetic coupling.

An interesting feature observed in all of the mechanically alloyed samples is the continued decrease of the resistivity in applied fields greater than that needed to saturate the magnetization, demonstrated for the $Co_{30}Ag_{70}$ sample milled for 130 h at low energy in figure 9. This behaviour is consistent with the picture of a metastable solution of Co dissolved in Ag since, while such Co atoms will not contribute much to the magnetization during their slow approach to saturation, they may contribute appreciably to the magnetoresistance.

Another possible explanation for the slow approach to saturation of the magnetoresistance has been suggested by Gehring *et al* [18], based upon the effects of a finite spin diffusion length (SDL) on the saturation of the magnetoresistance. In the ideal case of an

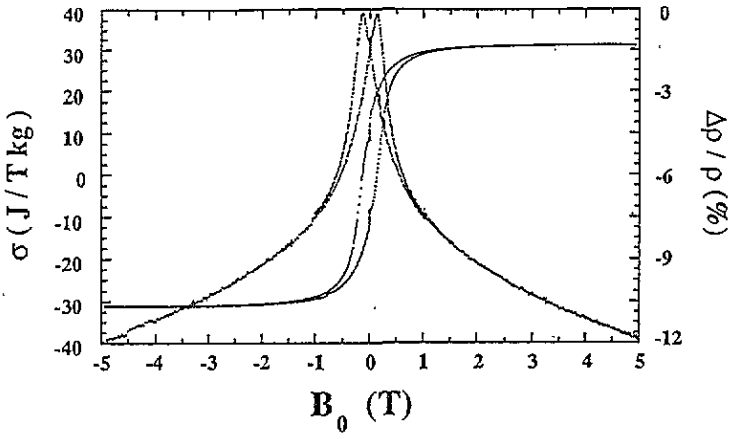

Figure 9. The 4.2 K magnetization and magnetoresistance curves of the $Co_{30}Ag_{70}$ sample milled at low energy for 130 h, demonstrating the continued decrease of the resistivity in fields greater than that sufficient to saturate the magnetization.

infinite SDL, both the magnetization and the magnetoresistance saturate in the same field. However, for real physical systems, which possess a finite SDL, the MR curves have a broadened full width half maximum value, with the tails of these curves asymptotically approaching the minimum resistivity given by the infinite SDL case. In the materials under investigation here, there is an additional contribution to the width of the MR curves deriving from a reduction of the SDL below that expected from a purely elemental point of view. This arises from the non-zero slope of the magnetization curve at high fields, corresponding to a small angle between neighbouring magnetic grains. In this case, a conduction electron may leave a particular magnetic grain with its spin parallel to the moment on that grain, but on reaching the next grain (which is at an angle of, say 2° to the first one) it will precess about the moment on this second grain, and can subsequently leave the vicinity of this second grain with its spin direction altered by up to 4° from its initial direction. Thus the electron spin direction will tend to deviate further and further from its initial direction as the electron traverses an increasing number of grains, until a point is reached where the spin direction effectively flips. This would have the effect of shortening the SDL, and consequently leading to the high-field behaviour seen in the magnetoresistance curves of figures 8 and 9.

Two different physical processes participate in the magnetoresistance measured in these magnetic systems: the GMR and the AMR. The latter is usually neglected as the GMR is normally more than ten times larger. However, in our mechanically alloyed samples where the GMR is not very large, it is possible to separate the two contributions. Using the fact that the GMR effect is isotropic and the AMR variation changes sign when the measurements are carried out parallel or transverse to the current, we have shown that it is possible to separate the two contributions by summing and subtracting the transversal and longitudinal curves and dividing by two [19]. This data treatment was carried out for the high-energy milled $Co_{30}Ag_{70}$ sample in figure 10. The observation that neither curve is saturated in 1.4 T indicates that both GMR and AMR effects are instrumental in the continued decrease of the resistivity in high fields. In fact, the analysis of these two contributions could aid in the description of the physical processes involved in the electronic transport properties of these granular systems. It is interesting to compare these two quantities since they both come from transport measurements (as opposed to comparing

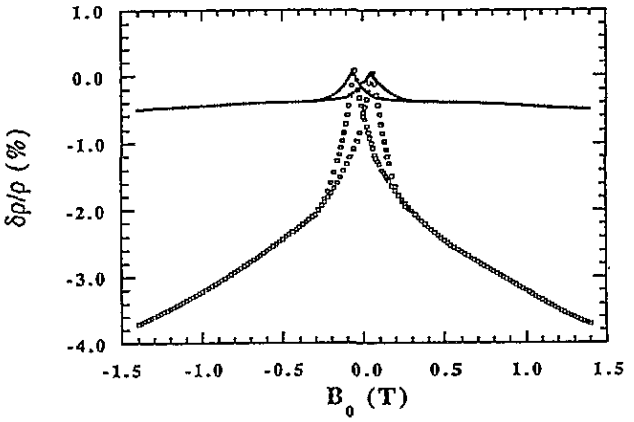

Figure 10. A plot of the GMR and the AMR for the $Co_{30}Ag_{70}$ sample milled at high energy.

GMR and magnetization for example). In the superparamagnetic regime, we can express the AMR contribution as a function of the applied field, knowing that spin–orbit scattering leads to a resistivity proportional to the square of the angle between the current and the local magnetization [6]: $\rho = \rho_\perp(\rho_\parallel - \rho_perp)\cos^2\theta$ with $\rho_\parallel$ and $\rho_\perp$ the resistivities with the current parallel or perpendicular to the magnetization. We then derive, for the AMR effect of a superparamagnetic system, that the extra resistivity due to the external field H applied along the current direction can be expressed as follows:

$$\Delta\rho_{AMR} = (\rho_\parallel - \rho_\perp)\left[\left(1 + \frac{2}{\alpha^2}\right) - \frac{2}{\alpha}\coth(\alpha)\right] \tag{1}$$

where $\Delta\rho_{AMR} = \rho - \rho_\perp$ and $\alpha = (\mu B_0)/(kT)$.

For the GMR contribution, it has been shown that:

$$\Delta\rho/\rho \propto (M/M_s)^2 \tag{2}$$

with M_s the saturation magnetization. AMR and GMR should then be proportional for sufficiently large α. As shown on figure 11, the linear law works well at high fields but not at low magnetization where the two sets of curves (B_0 increasing and B_0 decreasing) do not superimpose. In particular, the straight line does not extrapolate to zero as predicted by the model. However, this can be understood since the zero of the AMR is defined as the state where the directions of individual magnetization are random (in the pure superparamagnetic case this happens at zero field). In our samples, the bigger Co particles are likely to be multidomain at H_c; 180° domains would shift the origin we took for the AMR. Therefore, the absolute value of the AMR should be shifted by a small amount corresponding to the contribution of such multidomain particles, in which case the straight line at high fields should extrapolate to zero. This effect does not change the shape of the curve significantly. Also, the grains larger than the spin diffusion length of the conduction electrons in Co are thought to contribute significantly less to the GMR. Therefore, the AMR varies faster near H_c because the big grains are the ones which see their magnetization change at low field. The slope of the high-field fit gives a factor of 9.6 between GMR and AMR scattering cross sections in our samples.

Any increase in the average grain size (by annealing, for example) would tend to reduce the number of grains contributing to the GMR, and hence the GMR itself. Given the broad grain size distribution induced by the milling process, this may provide an explanation for

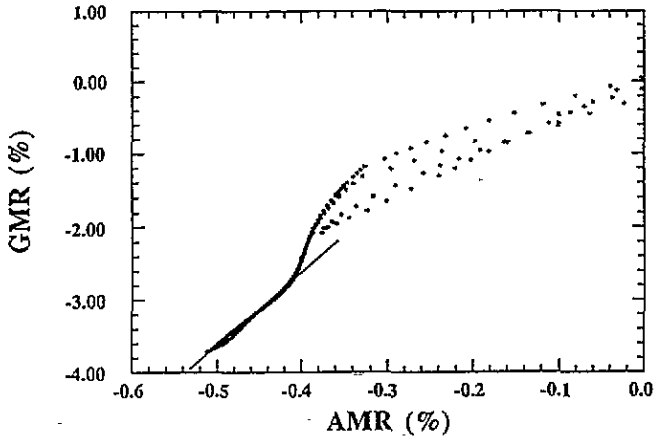

Figure 11. A plot of the GMR versus the AMR, showing the linear relationship at high field (or large negative GMR).

the relatively low GMR found in our mechanically alloyed materials, together with the subsequent decrease in the room temperature GMR after annealing, compared to that found in sputtered thin films of Co–Ag [17]. The relatively large residual resistivity further reduces the GMR through a larger non-magnetic contribution to the scattering.

The benefits of milling at a lower energy are reflected in the magnitude of the GMR of the $Co_{30}Ag_{70}$ sample milled for 130 h, which equalled that of the same composition milled at high energy, despite a microstructure which suggests that only about half of this sample contributes to the GMR. Furthermore, the lack of interactions between the Co grains suggests that a narrower grain size distribution, shifted to smaller sizes, exists for the fully mixed homogeneous regions, with a consequently higher proportion of the Co grains in these regions contributing to the GMR compared to the high-energy milled materials. On the basis of this observation, together with the concomitant reduction in the non-magnetic contribution to the scattering, it is reasonable to expect that larger effects may be achieved if one succeeds in fully homogenizing the entire sample on a micron-scale, either by milling for longer times, or by milling at an intermediate energy.

5. Conclusions

We have suggested that a metastable solid solution of Co in Ag surrounds the Co grains in the form of a halo. This feature should be studied by transmission electron microscopy to establish its effect on the GMR. Such a solid solution is not expected to be beneficial to the magnitude of the GMR (its effect should be similar to the scattering found in dilute magnetic alloys). However, evidence here suggests that very small Co aggregates may play a beneficial role, since the magnitude of the GMR decreases with increasing Co particle size at higher annealing temperatures. It is worth noting that the modest values of GMR measured here are mainly due to the very large residual resistances of the samples, which is evidence for a large defect concentration in the mechanically alloyed samples. From the point of view of processing, the optimization of the GMR in mechanically alloyed materials must involve a compromise between homogenizing the nanostructure for low-energy milling conditions and the creation of excessive residual resistivity due to defects created at high milling energies. An ideal post-milling treatment would eliminate both strain and defects

without altering the nanostructure. The large grain size distribution in these materials further reduces the magnitude of the GMR. A cobalt concentration close to the percolation threshold of Co in Ag was found to be the best.

The magnitude of the magnetoresistance measured in mechanically alloyed materials allowed for the easy separation of the GMR from the AMR. The measured curves followed the calculations made for an ideal superparamagnetic system in which the GMR is proportional to the AMR at high field. It would be interesting to further exploit the relation between the AMR and the GMR, since the former is a bulk effect while the latter is probably due to both the surface and the volume of the Co particles. A systematic study of both effects could lead to a better understanding of the role of surface and bulk scattering on the magnetoresistance.

Acknowledgments

The authors would like to acknowledge K O'Donnel for her advice on the ball milling technique and J Gregg for helpful discussions on the magnetoresistance saturation mechanisms. M Viret acknowledges the award of an HCM post-doctoral fellowship from the EC.

References

[1] Berkowitz A E, Mitchell J R, Carey M J, Young A P, Zhang S, Spada E E, Parker F T, Hutten A and Thomas G 1992 *Phys. Rev. Lett.* **68** 3745
[2] Xiao J Q, Jiang J S and Chien C L 1992 *Phys. Rev.* B **46** 9266
[3] Baibich M N, Broto J M, Fert A, Nguyen Van Dau F, Petroff E, Etienne P, Creuzet G, Frederich A and Chazelas J 1988 *Phys. Rev. Lett.* **61** 2472
[4] Searle C W and Wang S T 1969 *Can. J. Phys.* **47** 2703
[5] de Gennes P G and Friedel J 1958 *J. Phys. Chem. Solids* **4** 71
[6] Xiao J Q, Jiang J S and Chien C L 1992 *Phys. Rev. Lett.* **68** 3749
[7] Tsoukatos A, Wan H, Hadjipanayis G C and Li Z G 1992 *Appl. Phys. Lett.* **61** 3059
[8] Wecker J, von Helmolt R, Schultz L and Samwer K 1993 *Appl. Phys. Lett.* **62** 1985
[9] Coey J M D, Fagan A J, Skomski R, Gregg J, Ounadjela K and Thompson S M 1994 *IEEE Trans. Magn.* **30** 666
[10] Cugat O, Byrne R, McCauley J and Coey J M D 1994 *Rev. Sci. Instrum.* **65** 3570
[11] van der Pauw L J 1958 *Philips Res. Rep.* **13** 1–9
[12] Chikazumi S 1964 *Physics of Magnetism* NY
[13] Stearns M B and Cheng Y 1994 *J. Appl. Phys.* **75** 6894
[14] Holody P, Steren L B, Morel R, Fert A, Loloee R and Schroeder P A 1994 *Phys. Rev.* B **50** 12 999
[15] Ounadjela K, Herr A, Poinsot R, Coey J M D, Fagan A J, Staddon C R, Daniel D, Gregg J F, Thompson S M, O'Grady K and Greaves S 1994 *J. Appl. Phys.* **75** 6921
[16] Gregg J F, Thompson S M, Dawson S J, Ounadjela K, Staddon C R, Hammon J, Fermon C, Saux G and O'Grady K 1994 *Phys. Rev.* B **49** 1064
[17] Wang J-Q and Xiao G 1994 *Phys. Rev.* B **49** 3982
[18] Gehring G A, Gregg J F, Thompson S M and Watson M L 1995 *J. Magn. Magn. Mater.* **140–144** 501
[19] Viret M, Vignoles D, Cole D, Coey J M D, Allen W, Daniel D and Gregg J F to be published